Measurements of the breakup and neutron removal cross sections for ^{16}C

N. I. Ashwood,[1] M. Freer,[1] J. C. Angélique,[2] V. Bouchat,[3] W. N. Catford,[4,2] N. M. Clarke,[1] N. Curtis,[1] O. Dorvaux,[5] F. Hanappe,[3] Y. Kerckx,[3] M. Labiche,[6] J. L. Lecouey,[2,*] F. M. Marqués,[2] T. Materna,[3] A. Ninane,[7] G. Normand,[2] N. A. Orr,[2] S. Pain,[4,†] N. Soić,[1,‡] L. Stuttgé,[5] C. Timis,[2,§] A. Unshakova,[8] and V. A. Ziman[1]

[1]*School of Physics and Astronomy, University of Birmingham, Edgbaston, Birmingham, B15 2TT, United Kingdom*
[2]*Laboratoire de Physique Corpusculaire, ISMRA and Université de Caen, IN2P3-CNRS, 14050 Caen Cedex, France*
[3]*Université Libre de Bruxelles, CP 226, B-1050 Bruxelles, Belgium*
[4]*School of Electronics and Physical Sciences, University of Surrey, Guildford, Surrey GU2 7XH, United Kingdom*
[5]*Institut de Recherches Subatomique, IN2P3-CNRS/Université Louis Pasteur, Boîte Postale 28, 67037 Strasbourg Cedex, France*
[6]*Department of Electronic Engineering and Physics, University of Paisley, Paisley PA1 2BE, United Kingdom*
[7]*Institut de Physique, Université Catholique de Louvain, Louvain-la-Neuve, Belgium*
[8]*Joint Institute for Nuclear Research, 141980, Dubna, Moscow Region, Russia*

(Received 19 July 2004; published 14 December 2004)

Measurements of the breakup and the neutron removal reactions of ^{16}C have been made at 46 MeV/A and the decay cross sections measured. A correlation between the cluster breakup channels and the reaction Q value suggests that the reaction mechanism is strongly linked to quasielastic processes. No enhancement of the two-body cluster breakup cross section is seen for ^{16}C. This result would indicate that ^{16}C does not have a well developed cluster structure in the ground state, in agreement with recent calculations.

DOI: 10.1103/PhysRevC.70.064607 PACS number(s): 25.70.Pq, 25.70.Mn, 25.40.Hs, 25.60.Dz

For the most part, the structure of nuclei close to the neutron dripline has yet to be fully understood. It is, however, known that the properties of these nuclei will be heavily influenced by the weak binding of the valence neutrons. Studies of halo nuclei, such as ^{11}Li and ^{11}Be, show that weakly bound valence neutrons in low angular momentum orbits produce spatial wave functions which extend far from the core. It has been suggested by Horiuchi [1] that in order to maximize the binding of the valence neutrons at the driplines, ground-state nuclei must maximize the overlap of these neutrons with the protons contained in the core. In order to do this, the core can either deform or, optimally, form clusters, thus maximizing the surface area of the core seen by the valence neutrons. Studies of the odd mass boron nuclei $^{11\text{-}19}$B [2] show that this picture of a highly clustered core sitting in a cloud of weakly bound valence neutrons holds for those nuclei closest to the dripline.

Furthermore, Antisymmeterized Molecular Dynamics (AMD) calculations of the fragmentation of ^{13}B and ^{19}B by Takemoto [3] suggest that measurements of the cluster breakup cross sections can be used to indicate, qualitatively, the extent of clustering in the ground states of nuclei. Indeed, recent measurements of the cluster breakup cross sections of the neutron-rich nuclei ^{10,11,12,14}Be by Ashwood *et al.* [4] have indicated that the degree of clusterization in the ground state does not change between these nuclei, i.e., clusterization is important across the isotopic chain. This is in line with the most recent AMD calculations of Kanada-En'yo [5]. Furthermore, a comparison of the cluster breakup and neutron removal cross section of ^{14}Be and ^{14}B [6] shows an enhancement in the contribution of the two-body cluster breakup of ^{14}Be to the direct breakup process. This is in good agreement with the AMD calculations [2,7] for ^{14}Be and ^{14}B, which suggest that ^{14}Be has a more clustered ground state than ^{14}B.

Less is known about clustering in the neutron-rich carbon isotopes. AMD calculations [7] show the well known 3-α "trimer" configuration of ^{12}C. As the mass number increases, the neutron distribution extends further from the core, however there is very little change in the core proton density. von Oertzen [8] has predicted that levels in ^{16}C should even possess a well developed linear chain structure, however breakup measurements have so far been unable to confirm the presence of an α:2n:α:2n:α structure in ^{16}C [9,10].

This paper describes measurements of the breakup of a parasitic ^{16}C beam produced during an experiment, performed at GANIL, described in [6]. In this experiment, a secondary beam of ^{14}B was produced at 40.8 MeV/A by fragmentation of a 63 MeV/A ^{18}O primary beam on a rotating ^{9}Be target. A secondary parasitic beam of ^{16}C was also produced at ~3% of beam purity with an energy of 46 MeV/A and intensity on the order of 300 particles per second. Particle identification was achieved via time-of-flight through the LISE spectrometer.

The beam was tracked onto a 275 mg cm^{-2} carbon target using two drift chambers. A zero degree telescope, consisting of two orthogonal strip detectors and a close packed array of 16 CsI detectors, was used to detect the beam and reaction products. Neutrons produced in the reactions were detected using the DéMoN array, which consists of ~100 liquid scintillators. Angular ranges and detection efficiencies for both

*Present address: NSCL, Michigan State University, MI 48824.
†Present address: Department of Physics, Rutgers University, Newark, NJ 07102.
‡Present address: Rudjer Bošković Institute, Bijenička 54, HR-10000 Zagreb, Croatia.
§Present address: School of Electronics and Physical Sciences, University of Surrey, Surrey, GU2 7XH, United Kingdom.

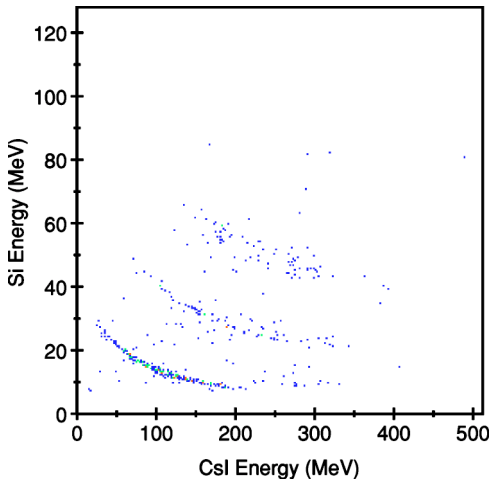

FIG. 1. (Color online) Particle identifiaction spectra (Si energy versus CsI energy) gated on ^{16}C in time-of-flight.

the zero degree telescope and neutron array can be found in [4,6].

Particle identification (PI) of reaction products was achieved using the EΔE technique. An example plot can be seen in Fig. 1 which is gated on ^{16}C in time-of-flight. Further PI spectra can be seen in Figs. 1 and 8 in Ref. [6], where identification of the ^{16}C beam can be seen at high energies in Fig. 8. The pixillation of the detector allowed the energy, mass, charge, and emission angle, and thus the momenta, of the reaction fragments to be calculated and the kinematics reconstructed. Rejection of particles resulting from the breakup of the ^{14}B beam was achieved in software by gating on the ^{16}C peak in the time-of-flight spectrum.

The excitation energy of the projectile prior to breakup was reconstructed by measuring the relative energy between the breakup particles and where the excitation energy, E_x, is given by $E_x = E_{thresh} + 1/2\,\mu v_{rel}^2$, where E_{thresh} is the threshold for the decay process (e.g., in $^{16}\mathrm{C} \rightarrow {}^{10}\mathrm{Be} + {}^{6}\mathrm{He}$, $E_{thresh} = 16.505$ MeV), μ is the reduced mass of the system, and v_{rel} is the relative velocity of the breakup particles. However, it is also possible to reconstruct the excitation energy of a projectilelike nucleus which is excited above the cluster breakup threshold, after neutron (or proton) emission/transfer from the projectile. This is discussed in more detail in [4,6].

Reconstruction of the ^{10}Be+^{6}He decay channel produced little yield in the excitation energy spectrum as shown in Fig. 2(a). However, knowledge of the efficiency, target thickness, and number of beam nuclei (measured using a PPAC at the entrance of the reaction chamber) gave a cross section for this channel of 200(190) μb. This compares with previously measured cross sections of 14.9(2.9) μb for the $^{10}\mathrm{Be}_{g.s} + {}^{6}\mathrm{He}_{g.s}$ channel [9] at an energy of 31.4 MeV/A. The difference in these measurements may be ascribed to the fact that in the latter experiment, only yield in the vicinity of the beam energy less the reaction Q value was selected for the calculation of the cross section. No coincidences for the ^{8}Li+^{8}Li breakup of the projectile were observed.

In the majority of channels, no significant structure was seen in the excitation energy spectra. In most cases this is a reflection of the very small cross sections involved. However, where significant yield was seen in the spectrum, the lack of structure could be attributed to the decay proceeding from regions with a high density of states, coupled with a reduced excitation energy resolution of $\sim$1 MeV, as well as the superposition of levels populated by breakup particles in different final states. It is also possible that reaction products in unbound states may contribute to the decay channel. For instance, the decay of ^{10}Be+^{6}He* may contribute to the ^{10}Be+^{4}He channel through 2n emission from ^{6}He (direct breakup of the ^{16}C projectile may occur but the phase space for this is very small). The associated excitation energy spectrum for this channel is shown in Fig. 2(b).

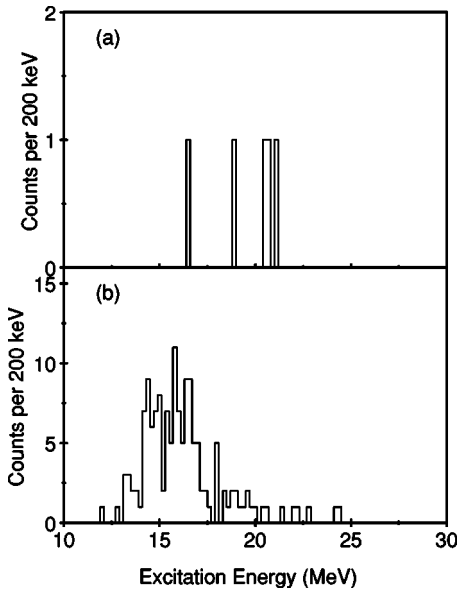

FIG. 2. Excitation energy spectra for (a) the ^{10}Be+^{6}He breakup channel and (b) the ^{10}Be+^{4}He breakup channel.

Only one channel showed any significant structure in the excitation energy spectrum and that corresponds to that for ^{4}He+^{4}He coincidences. Figure 3 shows the total energy spectrum for this channel. Here the total energy, E_{tot}, is given by $E_{\alpha_1} + E_{\alpha_2} + E_{recoil}$ and $E_{tot} = E_{beam} + Q_3$, where Q_3 is the three-body reaction Q value and E_{recoil} has been reconstructed from momentum conservation. In the case of inelastic scattering followed by the breakup of ^{16}C* into ^{4}He

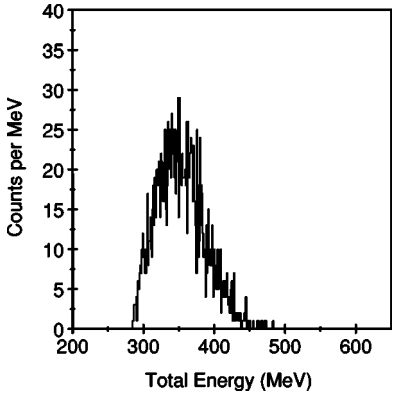

FIG. 3. Total energy spectrum for the ^{4}He+^{4}He breakup channel.

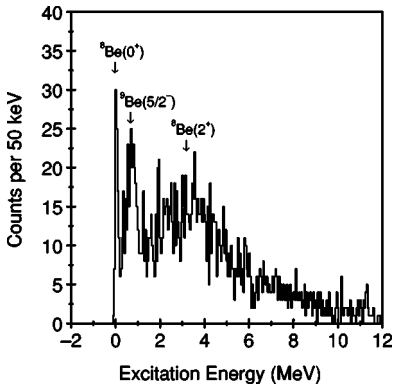

FIG. 4. The excitation energy spectrum corresponding to $\alpha+\alpha$ coincidences. The peaks at ~100 keV and ~3 MeV correspond to decays to the ground and 2^+ states of ^{8}Be. The peak at ~800 keV is produced by the decay of the 2.43 MeV $(5/2^-)$ state in ^{9}Be to the low-energy tail of the 2^+ state in ^{8}Be.

$+^4$He where both the target and the recoil are in their ground states, yield would lie in the region ~650 MeV, taking into account energy straggling of the beam in the target. Figure 3 clearly shows that this is not the case and would indicate that a more complex reaction is taking place where it is possible that both ejectile and the target recoil do not stay intact. Figure 4 shows the associated excitation energy spectrum for the ^{4}He+^{4}He channel. Both the ground state and the 2^+ (3.06 MeV) state in ^{8}Be are populated along with a peak at ~800 keV. This is not a state in ^{8}Be, but is consistent with the decay process proceeding via the $5/2^-$ (2.43 MeV) state in ^{9}Be, which then decays through the low-energy tail of the ^{8}Be, 2^+ [4,6,11,12]. From this observation, a lower limit of the cross section to ^{9}Be can be found.

Cross sections for all the decay channels studied are listed in Table I. Coincidences between three α particles were also reconstructed, however no yield was seen in this channel, or any other three-body cluster decay channels in these data. The uncertainties quoted are purely statistical. Systematic errors in the determination of the cross section come from the uncertainty in the nature of the angular distributions used in the Monte Carlo simulations. These are estimated to be ~20%. Cross sections for the emission of neutrons from the carbon isotopes were measured by detecting a carbon nucleus in coincidence with a single neutron and then fitting the neutron angular distribution with a Lorentzian line shape and integrating over the angular range. This is further described in [4,6]. A background subtraction was performed using data from a target out run. A one-neutron removal cross section of 96(11) mb was measured for the decay of ^{16}C. This is in very good agreement, along with the two-neutron removal cross section of 94(11) mb, with previous measurements [13–15], although the present data have been measured at a lower energy.

Figure 5 shows the ^{x}C+1n and cluster breakup cross sections versus mass of the detected fragment. The measurement of the multineutron removal channels via the coincident detection of a charged particle and a single neutron presents the advantage that the detection efficiency is not prohibitively small. In this case, the true cross section for the

TABLE I. Cross sections for the reactions with the ^{16}C beam. The ^{x}Li+^{y}Be, ^{x}He+^{y}Be, ^{x}Li+^{y}Li, ^{x}He+^{y}Li, and ^{x}He+^{y}He channels were measured by coincident detection of the two charged fragments, while the cross sections for the ^{x}C+1n channels were measured by detecting the fragment and the single neutron in coincidence. Upper limits are given for channels were no yield was seen after background subtraction.

Channel	σ(b)	Channel	σ(b)
^{15}C+1n	0.096(0.011)	^{9}Li+^{8}He	$<70\times10^{-6}$
^{14}C+1n	0.094(0.011)	^{9}Li+^{6}He	$200(190)\times10^{-6}$
^{13}C+1n	0.033(0.004)	^{9}Li+^{4}He	0.002(0.001)
^{12}C+1n	0.011(0.001)	^{8}Li+^{8}Li	$<70\times10^{-6}$
^{10}Be+^{10}Be	$<70\times10^{-6}$	^{8}Li+^{7}Li	$550(360)\times10^{-6}$
^{10}Be+^{9}Be	$<70\times10^{-6}$	^{8}Li+^{6}Li	$140(150)\times10^{-6}$
^{10}Be+^{9}Li	$<70\times10^{-6}$	^{8}Li+^{8}He	$<70\times10^{-6}$
^{10}Be+^{8}Li	$<70\times10^{-6}$	^{8}Li+^{6}He	$480(330)\times10^{-6}$
^{10}Be+^{7}Li	$70(100)\times10^{-6}$	^{8}Li+^{4}He	0.010(0.003)
^{10}Be+^{6}Li	$<70\times10^{-6}$	^{7}Li+^{7}Li	$680(420)\times10^{-6}$
^{10}Be+^{8}He	$<70\times10^{-6}$	^{7}Li+^{6}Li	$890(510)\times10^{-6}$
^{10}Be+^{6}He	$200(190)\times10^{-6}$	^{7}Li+^{8}He	$340(270)\times10^{-6}$
^{10}Be+^{4}He	0.015(0.004)	^{7}Li+^{6}He	0.001(0.001)
^{9}Be+^{9}Be	$<70\times10^{-6}$	^{7}Li+^{4}He	0.032(0.008)
^{9}Be+^{9}Li	$<70\times10^{-6}$	^{6}Li+^{6}Li	$<70\times10^{-6}$
^{9}Be+^{8}Li	$<70\times10^{-6}$	^{6}Li+^{8}He	$410(300)\times10^{-6}$
^{9}Be+^{7}Li	$270(230)\times10^{-6}$	^{6}Li+^{6}He	$340(270)\times10^{-6}$
^{9}Be+^{6}Li	$70(100)\times10^{-6}$	^{6}Li+^{4}He	0.012(0.004)
^{9}Be+^{8}He	$70(100)\times10^{-6}$	^{8}He+^{8}He	$140(150)\times10^{-6}$
^{9}Be+^{6}He	$410(300)\times10^{-6}$	^{8}He+^{6}He	$820(480)\times10^{-6}$
^{9}Be+^{4}He	0.013(0.004)	^{8}He+^{4}He	0.003(0.001)
^{9}Li+^{9}Li	$<70\times10^{-6}$	^{6}He+^{6}He	$750(450)\times10^{-6}$
^{9}Li+^{8}Li	$<70\times10^{-6}$	^{6}He+^{4}He	0.010(0.003)
^{9}Li+^{7}Li	$<70\times10^{-6}$	^{4}He+^{4}He	0.131(0.025)
^{9}Li+^{6}Li	$<70\times10^{-6}$	^{4}He+^{4}He+^{4}He	$<105\times10^{-6}$

$A-$Xn channel should be reduced by a factor X. However, the neutron angular distributions vary at each decay step, and, moreover, the multiplicity of the emitted neutrons does not necessarily equal the number of missing neutrons, with the possibility of projectile neutrons interacting strongly with the target [16]. For the sake of comparison with the cluster breakup cross section, the neutron removal cross sections have been normalized at each step by dividing by X. From Fig. 5, it is seen that the neutron removal cross section steadily decreases over each step. It is also the dominant decay process over the first two steps, i.e., the decay of nuclei with $A=16$ and 15. However, unlike the breakup of the Be isotopes and ^{14}B measured in [4,6], the neutron decay is not the dominant decay over all steps. The measured cross sections indicate that the decay of ^{14}C is more likely to proceed via cluster breakup than by neutron emission. This could be associated with a large neutron separation energy for ^{14}C of 8.2 MeV along with the ^{14}C being able to decay through several two-body breakup channels.

For the cluster breakup of the C, B, and Be fragments, the

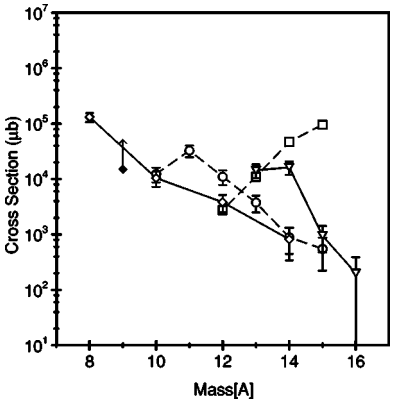

FIG. 5. ^{x}B+1n cross sections (squares) and cluster breakup cross sections from C (triangles), B (circles), and Be (diamonds) versus the mass of the decay fragment for the ^{16}C beam. The neutron removal channels are normalized by dividing by the difference in the number of neutrons between the observed fragment and the projectile. Closed symbols represent lower limits.

cross sections steadily increase with decreasing mass. This is consistent with the cross section/mass systematics seen with beams of ^{10,11,12,14}Be [4] and ^{14}B [6]. The majority of the summed total cluster breakup cross section, ~55% or 0.131(0.025) b, is associated with the ^{4}He+^{4}He channel, which was also seen in [4,6]. However, it should be noted that only a lower limit in the cross section could be measured for the decay to ^{9}Be and so an increase in this cross section should be expected.

The decay process, for example via the ^{4}He+^{4}He channel, could be reached by several different reaction mechanisms. These could range from a direct reaction mechanism, whereby the ^{16}C is excited to an unbound state above the decay threshold, to a single-step decay from the composite system formed by the projectile and target (in this case ^{28}Mg). It is also possible that each channel may be fed by a sequence of decays from unbound states in the decay fragments. Plotted in Fig. 6 are the measured cross sections versus the decay threshold in ^{16}C to the channels listed in Table

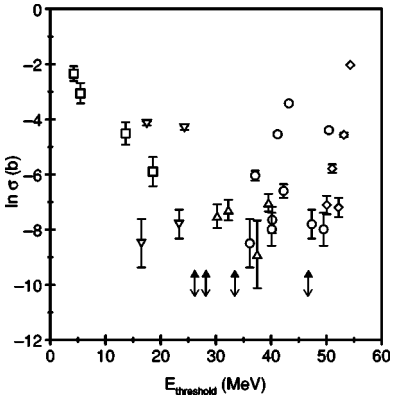

FIG. 6. Plot of ln(σ) versus the decay-energy threshold in the projectile nucleus ^{16}C. The squares show the ^{x}C+1n cross sections. The breakup into ^{x}Be+^{y}He is indicated by triangles, ^{x}Li+^{y}Li is indicated by deltas, ^{x}Li+^{y}He is indicated by circles, and diamonds represent the ^{x}He+^{y}He breakup.

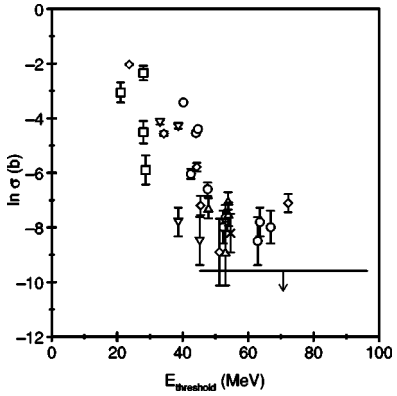

FIG. 7. Plot of ln(σ) versus the decay-energy threshold in the compound nucleus ^{28}Mg. The squares show the ^{x}C cross sections. The breakup into ^{x}Be+^{y}Li is indicated by crosses, ^{x}Be+^{y}He is indicated by triangles, ^{x}Li+^{y}Li is indicated by deltas, ^{x}Li+^{y}He is indicated by circles, and diamonds represent the ^{x}He+^{y}He breakup. The horizontal line represents the range in energy for channels where only an upper limit in the cross section could be found.

I. There does seem to be a correlation for the neutron removal cross section; this is seen to have an exponential trend. There is, however, little correlation between threshold energy and cluster breakup cross sections. Indeed, the cluster decay channel with the highest cross section is the ^{4}He +^{4}He channel, which has the highest decay threshold. Even if this channel is produced by a series of sequential decays (e.g., two-proton emission from ^{16}C to ^{14}Be followed by six-neutron decay to ^{8}Be), the ^{16}C must be excited to 54.34 MeV and thus make it unfavored over the two-body decay ^{10}Be +^{6}He, which has a decay threshold of 16.51 MeV. The phase space [4,6,17–19] for multiparticle decays is also highly constrained compared to that of two-body cluster breakup. It is therefore unlikely that the ^{4}He+^{4}He channel is populated via the inelastic excitation of the beam to unbound states above the decay threshold for this channel. It could also be possible that the ^{4}He+^{4}He channel is populated after proton transfer from the projectile, however this would mean that all other favorable decay channels, i.e., those with lower decay thresholds, must be suppressed.

It is possible that higher-order mechanisms play a part in the reaction process. Figure 7 shows a plot of cross section versus decay threshold for each channel from the composite system (e.g., $^{28}\mathrm{Mg}\rightarrow{}^{10}\mathrm{Be}+{}^{6}\mathrm{He}+{}^{12}\mathrm{C}$; E_{thresh}=45.22 MeV or $^{28}\mathrm{Mg}\rightarrow{}^{15}\mathrm{C}+{}^{13}\mathrm{C}$; E_{thresh}=28.017 MeV). In all cases the thresholds have been calculated assuming that all possible excess neutrons and protons in the reaction have been carried off by the undetected charged particle. Figure 7 shows that there is now a correlation between the cross section and the threshold energy for most of the reaction channels, including that for ^{4}He+^{4}He. Indeed, decay for a composite state may now explain how the ^{8}Be may be populated without the need for the suppression of other more likely reaction channels and why the excitation energy spectrum has no large contribution from $\alpha+\alpha+X$ decay for nuclei other than ^{8}Be, that is to say that the ^{8}Be nucleus is produced directly and there are few α-α coincidences which arise from other sources.

The decay velocities of the breakup particles were mea-

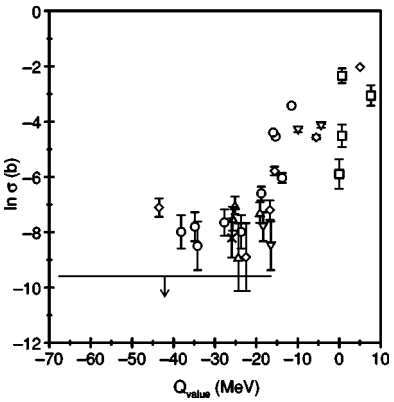

FIG. 8. Plot of ln(σ) versus the reaction Q value for a ^{16}C projectile and ^{12}C target. The squares show the ^{x}C cross sections. The breakup into ^{x}Be+^{y}Li is indicated by crosses, ^{x}Be+^{y}He is indicated by triangles, ^{x}Li+^{y}Li is indicated by deltas, ^{x}Li+^{y}He is indicated by circles, and diamonds represent the ^{x}He+^{y}He breakup. The horizontal line represents the range in energy for channels where only an upper limit in the cross section could be found.

sured. For lithium and helium isotopes, a large spread of velocities were measured ranging between the beam velocity and the center-of-mass velocity, which suggests, like those measured in [6], that the reaction mechanism may be quasielastic, i.e., there may be some exchange of nucleons between target and projectile. Thus, the cross sections have been plotted against the reaction Q value in Fig. 8. In both Figs. 7 and 8, there are some data points which seem to lie off the general trend of the data. These are related to the ^{8}He+^{7}Li and ^{6}He+^{9}Li decay after one-proton removal, ^{8}He +^{6}Li after deuteron removal, and most notably the ^{8}He +^{6}He decay of ^{14}Be after two-proton removal. These would suggest that, as one may expect, there is a large direct reaction contribution to the reaction process in these cases. It is also interesting to note that the two-body cluster breakup of the ^{16}C beam does not seem to have an enhanced direct contribution, which would indicate, from the AMD calculations of Takemoto [3], that the ground state of ^{16}C does not have a strong cluster structure. This would be in agreement with the AMD calculation of Kanada-En'yo *et al.* [5].

In summary, measurements of the breakup of ^{16}C have been made at 46 MeV/A. The coincident detection of the decay products allowed the excitation energies of the projectilelike nuclei to be reconstructed. The excitation spectrum for ^{4}He+^{4}He decay of ^{8}Be suggests that a large fraction of the reaction flux proceeds via the emission of a ^{8}Be nucleus. Although little structure was seen in the excitation energy spectra, in most channels the cross sections could be measured. The measured cross sections cannot be understood entirely in terms of the direct breakup of the projectile nucleus, however there appears to be a correlation between the cluster breakup channels and the decay thresholds in the compound nuclear system (^{28}Mg) and reaction Q value. The velocity distributions indicate that the dominant processes are quasielastic in nature. Enhancement of decay channels which occur after one- and two-proton emission suggests that there may be some direct contribution to these reactions, however these results also indicate that ^{16}C does not have a well developed cluster structure in its ground state, in agreement with AMD calculations [7].

The authors are grateful to the technical and operations staff of LPC and GANIL for help in preparing and performing the experiments described here. This work was funded by the EPSRC (UK) and the IN2P3-CNRS (France). Additional support was provided by the Human Capital and Mobility Program of the European Community (Contract No. CHGE-CT94-0056).

[1] H. Horiuchi, *Proceedings of the 7th International Conference on "Clustering Aspects of Nuclear Structure and Dynamics"* (World Scientific, Singapore, 2000), p. 405.
[2] Y. Kanada-En'yo and H. Horiuchi, Phys. Rev. C **52**, 647 (1995).
[3] H. Takemoto, H. Horiuchi, and A. Ono, Phys. Rev. C **63**, 034615 (2001).
[4] N. I. Ashwood *et al.*, Phys. Lett. B **580**, 129 (2004).
[5] Y. Kanada-En'yo and H. Horiuchi, Phys. Rev. C **68**, 014319 (2003).
[6] N. I. Ashwood *et al.*, Phys. Rev. C **70**, 024608 (2004)
[7] Y. Kanada-En'yo and H. Horiuchi, Prog. Theor. Phys. Suppl. **142**, 205 (2001).
[8] W. von Oertzen, Z. Phys. A **357**, 355 (1997).
[9] P. J. Leask *et al.*, J. Phys. G **27**, 9 (2001).
[10] B. J. Greenhalgh *et al.*, Phys. Rev. C **66**, 027302 (2002).
[11] Y. S. Chen *et al.*, Nucl. Phys. **A146**, 136 (1970).
[12] S. Ahmed *et al.*, Phys. Rev. C **69**, 024303 (2004).
[13] E. Sauvan *et al.*, Phys. Rev. C **69**, 044603 (2004).
[14] V. Maddalena *et al.*, Phys. Rev. C **63**, 024613 (2001).
[15] T. Yamaguchi *et al.*, Nucl. Phys. **A724**, 3 (2003).
[16] M. Labiche *et al.*, Phys. Rev. Lett. **86**, 600 (2001).
[17] E. Fermi, Prog. Theor. Phys. **5**, 1570 (1950).
[18] M. Kretschmar, Annu. Rev. Nucl. Sci. **11**, 1 (1961).
[19] M. Epherre and E. Gradsztajn, Rev. Phys. Appl. **18**, 48 (1967).